Indian Journal of Chemical Technology
Vol. 31, September 2024, pp. 691-701
DOI: 10.56042/ijct.v31i5.10906

Spectrophotometric quantification of biotin in drug formulations utilizing Pd(II) promoted ligand substitution approach in micellar medium

Abhishek Srivastava[1]*, Neetu Srivastava[2] &Vinay Kumar Singh[3]*

[1]Department of Chemistry, GLA University, Mathura, U.P., India
[2]Department of Chemistry, D.D.U. Gorakhpur University, Gorakhpur, U.P., India
[3]Department of Chemistry, University of Lucknow, Lucknow, U.P., India
*E-mail: aabhichem@gla.ac.in

Received 5 May 2024; accepted 8 July 2024

A spectrophotometric approach that is straightforward, efficient, highly sensitive, and precise has been devised for quantifying biotin in both its pure state and pharmaceutical samples. Analysis of biotin in biological and pharmaceutical samples is essential for therapeutic evaluation and patient follow-up bioavailability. Several methods for determining this drug have drawbacks including specialized equipment that many quality control laboratories and universities in developing countries lack. The methodology relies on the inhibitory approach of biotin on the Pd(II) promoted ligand substitution (LS) reaction involving phenylhydrazine (PHZ) and hexacyanoferrate(II). The process entails replacing cyanide in $[Fe(CN)_6]^{4-}$ with PHZ, triggering the development of a complex $[Fe(CN)_5PHZ]^{3-}$. The complex demonstrates a significant level of absorption at a specific wavelength of 488 nm. The established limit of detection for biotin is 0.117 μg mL^{-1}. Experiments on recovery are conducted to confirm the precision and accuracy of biotin quantification. The suggested approach has been effectively utilized for the examination of biotin in pristine samples and various medications, demonstrating remarkable levels of precision and accuracy. The outcomes show good agreement when compared to the findings of the official analytical method. The excipients typically employed in medicines do not exhibit any interference with the suggested methodology. This methodology is highly effective for accurately determining trace levels of different drugs and biological molecules that can significantly impede the catalytic efficiency of Pd(II).

Keywords: Biotin determination, Hexacyanoferrate(II), Inhibitory approach, Kinetic-spectrophotometric, Ligand substitution reaction, Pharmaceutical preparations

Introduction

Biotin is a water-soluble B-complex vitamin that is present in certain foods and can also be obtained through supplements. Biotin promotes the health of your eyes, hair, and skin, and also plays a crucial role in facilitating enzymes to metabolize proteins, carbohydrates, and fats in food[1,2]. Additionally, it aids in the regulation of cellular signaling and gene activity[3-4]. Notable dietary sources of biotin (BTN) with high levels include the pancreas, heart, kidneys, liver, milk, chicken, and egg yolk. Plants, primarily in their seeds, contain smaller amounts[5]. People in Western nations are thought to consume 35 to 70 mg of BTN per day through diet, with nearly that entire amount being absorbed[6]. For healthy adults, a daily intake of 35 mg of BTN through diet is deemed sufficient. Inadequate BTN ingestion has been documented to cause significant biochemical abnormalities in animal organisms, including decreased antibody production, suppression of protein and RNA synthesis, and diminished carboxylase activity[7-8]. Serious animal syndromes like the trout "blue slime", kidney syndrome and avian fatty liver disease appear to be linked to BTN deficiency[9]. Extended lack of BTN in the human body can result in the development of pathological symptoms that can be alleviated by the administration of BTN[7]. A deficiency in BTN has been linked to severe human disease states, such as Multiple Carboxylase Deficiency, an inherited metabolic syndrome[10]. There is also a correlation between BTN deficiency and various human malfunctions, such as Rett syndrome, Leiner disease, Seborrheic dermatitis of infancy, and Sudden Infant Death Syndrome[11].

Surfactants serve as vital constituents in pharmaceuticals as they are composed of both hydrophilic and hydrophobic groups. Surfactants find application in the pharmaceutical industry in various ways: (i) to facilitate the solubilization of hydrophobic drugs in aqueous solutions; (ii) to serve as constituents

of emulsions; (iii) functioning as plasticizers in semisolid delivery systems; (iv) to function as self-assembling vehicles for surfactant-based oral and transdermal drug delivery; and (v) employed as agents to enhance drug absorption and penetration[12, 13]. The surfactant's aqueous solution demonstrates electrolytic behavior when present in low concentrations. Micellization occurs in an aqueous environment due to the presence of a substrate containing hydrophobic as well as hydrophilic components. The concentration at which surfactants spontaneously generate micelles is referred to as the critical micelle concentration (CMC)[14]. Surfactant molecules display both attractive and repulsive interactions. It is intriguing to witness the aggregation of surfactant molecules into micelles of a variety of sizes and shapes once they surpass the CMC. The CMC of sodium lauryl sulfate (SLS), an anionic surfactant, at a temperature of 298 K varies between 8.0×10^{-3} M and 8.5×10^{-3} M[15-17]. When compared to pure solvents, reactants that are bound within micelles encounter a completely different reaction atmosphere. Understanding the factors that influence the reaction rate in a micellar medium is crucial. One of these factors is the extent of interaction between the substrate and the micelle aggregates.

For centuries, sulfur has consistently been the primary heteroatom in the extensive array of bioactive compounds, insecticides, and. Fungicides. In numerous processes of metabolism, organosulfur compounds play an essential role as enzymes or structural proteins[18-20]. Pharmaceutical companies are always on the lookout for analytical chemists who excel in developing cutting-edge technology to detect and measure sulfur-containing biologically active compounds and medications in a wide range of samples. Because of the fundamental significance and practicality of the ligand exchange and oxidation-reduction reactions of complexes consisting of transition metals in synthetic, organometallic, and analytical chemistry, a significant number of researchers have been motivated to investigate the kinetics of these processes[21-24]. Some authors have documented kinetic studies of nitrogen heterocyclic ligands substituting cyanide form $[Ru/Fe(CN)_6]$[4-25-27]. These approaches have additionally been deployed to effectively evaluate the employed catalysts and moieties that have a significant interaction with the catalyst[28-30].

Chromatographic approaches, such as capillary electrophoresis, have been extensively employed for the analysis of BTN in pharmaceutical samples[31]. Nevertheless, the practical use of several of these techniques is restricted by their lack of sensitivity[32]. Although HPLC can be valuable in analyzing low levels of BTN in basic substances, its procedure is quite complex. Before the determination can be made, BTN needs to be extracted or separated, which not only makes the process tedious but also raises the risk of potential errors[32]. Ultraviolet (UV) detection is a frequently utilized method in liquid chromatographic techniques. This involves measuring the absorbance of BTN after pre-column derivatization utilizing a suitable modifying reagent[33,34]. However, the procedures necessary for the separation of BTN before subsequent UV or colorimetric measurement are arduous and hectic[35]. Moreover, numerous laboratories are unable to employ these methods due to the substantial instrumental and operational expenses associated with them. Nevertheless, micellar electrokinetic capillary chromatography (MEKC) is an expensive method for quantifying BTN in biological and pharmaceutical samples[36]. Although spectrophotometric methods are relatively straightforward, one drawback is their limited selectivity[37]. This means that before carrying out the derivatization process through a condensation reaction, it is necessary to first separate the components, which can be quite time-consuming[37]. So, most of the methods described in scientific literature for measuring BTN are not very sensitive and involve complex sample preparation. They often require heating and extended cooling periods before analysis can be performed. Among the different methods used to determine this drug, there are several drawbacks to consider. These include the need for specialized equipment, which is often not readily accessible in many quality control laboratories and universities in developing countries[32]. Table 1 demonstrates the different physicochemical approaches for the determination of BTN.

The analysis of BTN in biological and pharmaceutical samples is crucial for understanding its therapeutic evaluation and bioavailability during patient follow-up. Regular testing by laboratories for medications in the market is crucial for safeguarding the public's well-being, particularly in developing nations where the widespread presence of spurious and substandard drugs presents a significant obstacle to healthcare services. Hence, there is an additional requirement for the advancement of uncomplicated, cost-effective, highly responsive, and precise techniques to evaluate the quality of pharmaceuticals available in the market. Due to the high cost associated with many reported methods, we have come up with an in-house ligand substitution kinetic assay for BTN. The utilization of this technique aligns with our continuous pursuit of

Table 1 — Comparative studies for the quantification of Biotin using different methods

Method	Description	Detection limit	Reference
HPLC-UV	C_{18} column was used	1.0 µg/mL	33
HPLC and micellar electrokinetic capillary chromatography (MEKC)	Study was performed in micellar medium	0.15 µg/mL	36
Kinetic Spectrophotometric	Utilizing biotin's catalytic impact on the tri-iodide-sodium azide reaction	0.15 µg/mL	37
Spectrofluorimetric	Used 4-fluoro-7-nitrobenzofurazan to derivatize biotin	0.038 ng/mL	38
RP-HPLC	Biotin was determined in multivitamin-multimineral tablets	Detection range: 0.5-2.0 µg/mL	39
TLC	Biotin was determined in the presence of all water-soluble vitamins	0.15 µg/ml	40
Kinetic spectrophotometric	Based on the inhibitory kinetic approach	Detection range: 0.031 - 1.466 µg mL^{-1}	This work

exploring analytical methodologies that depend on catalytic ligand substitution and oxidation reactions[26-30]. Our objective of the current research is to develop a highly sensitive, specific, fast, precise, and cost-effective methodology for quantifying BTN in both pure and pharmaceutical formulations. In addition, the existing methodology can also be used to determine other biomolecules that contain sulfur, as these molecules can significantly reduce the catalytic activity of Pd^{2+} by forming a strong complex with it. The experimental protocol relies on the inhibitory effect of BTN regarding the cyanide substitution from $[Fe(CN)_6]^{4-}$ with phenylhydrazine (PHZ), facilitated by Pd^{2+}.

Experimental Section

Reagents and chemicals

To prepare the solutions of the desired concentrations, AR grade palladium(II) chloride (Merck), Biotin (Himedia), sodium lauryl sulfate (Sigma-Aldrich), phenylhydrazine hydrochloride (Merck), and potassium hexacyanoferrate(II) (Merck) were utilized. The standard solution of 1.0×10^{-2} M BTN and 5.0×10^{-2} M potassium hexacyanoferrate(II) was prepared by precisely weighing their estimated quantities in double distilled de-ionized water. A dark amber-colored bottle was utilized to store the potassium hexacyanoferrate(II) solution in order to prevent photodegradation and oxidation. To ensure the pH of the reacting mixture remained at 3.25 ± 0.01, a phthalate buffer was employed. The pH meter was standardized using the standard BDH buffers prior to use. The ionic strength of the reaction mixture was maintained by employing sodium nitrate (Merck). The volumetric apparatus utilized in the current investigation was of certified 'A' grade and underwent regular steaming prior to its utilization. The hexacyanoferrate(II) and palladium(II) solutions were appropriately diluted prior to utilization in order to mitigate potential uncertainties arising from the adsorption of Pd^{2+} ions on glass and to prevent the photodegradation and oxidation of hexacyanoferrate(II).

Apparatus

The pH of the reaction mixture was regulated employing a Lab Junction pH Meter (model LJ-111), which was validated with a prescribed buffer solution. A double-beam T65 UV-visible spectrophotometer made by PG Instruments Limited was deployed for the acquisition of product absorption spectra and to measure absorbance at a specified wavelength. The self-designed circulating water arrangement system kept the cell compartment at a constant temperature.

Procedure

The indicator reaction was thoroughly studied kinetically before the experimental conditions were set. The reactant concentration and other parameters were chosen so that the reaction's initial rate and sensitivity demonstrated their maxima. The temperature during the experiments was 298K. Thus, the reactants were pre-immersed in a thermostat for 30 min to maintain their temperature at 298 ± 0.1 K during each kinetic run. The substitution reaction under investigation was conducted in an acidic environment, with the pH of all the reactants meticulously calibrated to 3.25 ± 0.01, which is considered the optimal value. In a volumetric flask, the reactants with specified concentrations were scrupulously mixed in a precise sequence. The PHZ, SLS, Pd^{2+}, and buffer were added first, followed by the substrate $[Fe(CN)_6]^{4-}$ solution, which was added just before each kinetic run. The reaction mixture was carefully transferred to a spectrophotometric cuvette with a 10 mm path length, ensuring it was properly

shaken. The cuvette was subsequently placed within a cell compartment that was regulated by temperature. The monitoring of the reaction progress involved determining the reaction's initial rate by computing a rise in absorbance corresponding to $[Fe(CN)_5PHZ]^{3-}$. The complex was generated as a result of the reaction and demonstrated pronounced absorption at a wavelength of 488 nm, with no disruption from the reacting agents[41,42]. The fixed time absorbance was utilized as a metric to optimize the relationship between the reaction variables and the initial rate. Under optimal circumstances, three calibration models were developed that involved the correlation between the absorbance at fixed times and reported [BTN]. The optimal conditions for quantifying [BTN] and in unknown samples were determined by preparing a series of solution specimens containing varying known levels of BTN, followed by recovery procedures. All the experiments were performed in triplicates.

Results and Discussion

The reaction occurring between PHZ and $[Fe(CN)_6]^{4-}$ is expedited by Pd^{2+}, resulting in the development of the anionic compound, $[Fe(CN)_5PHZ]^{3-}$. The regeneration of the catalytic species Pd^{2+} occurs in an acidic environment. Through the examination of the slope ratio and mole ratio of the finished product of the reaction, it has been ascertained that the reaction involving PHZ and $[Fe(CN)_6]^{4-}$ takes place in a mole ratio of 1:1. No modifications were implemented to the absorption measurements as, when the final reaction product was excluded, neither of the interacting solutions demonstrated noticeable absorption at the assessed wavelength. The aqueous solution of the formed complex is quite stable as no significant change in absorbance was noticed even after 5 days after the completion of reaction. Considering the strong stability of the final substitution product and the notable hindrance of BTN on the catalytic effectiveness of Pd(II), we have chosen to use this LS reaction for determining BTN.

Optimizationof the reaction variables

Influence of varying pH levels on the initial rate

The cyanide substitution from $[Fe(CN)_6]^{4-}$ with nitrogen donor ligands, regardless of whether it is uncatalyzed or catalyzed, has been demonstrated to be significantly affected by pH[27-30]. A fixed-time protocol was employed to explore the influence of pH on the rate of complex formation within the pH spectrum of 1.0 – 8.0. The pH levels were adjusted within the range of 1.0 - 8.0 by employing a phthalate buffer. At different pH levels, absorbance a measure of the initial rate was measured at 4, 7, and 10 min of reactant mixing.

The diagram illustrating the correlation between pH and absorbance (Fig. 1) illustrates the slow rate of the reaction at elevated $[H^+]$. It exhibits a consistent increase until pH 3.25, after which it decreases as the pH approaches 8.0. The pH value that is most favorable for quantifying BTN could be regarded as 3.25. The diminished rate observed at lower pH levels is believed to be due to the presence of a less reactive protonated state of $[Fe(CN)_6]^{4-}$ and PHZ. When the pH is increased, the compounds $[Fe(CN)_6]^{4-}$ and PHZ preferentially exist in their deprotonated form[43, 44]. The decreased rate observed at higher pH levels may be ascribed to the diminished availability of H^+ ions necessary for the rejuvenation of the catalyst Pd^{2+} (Ref.41).

Influence of varying [SLS] on the initial rate

All other parameters were held constant while [SLS] was altered from 2.0×10^{-3} M to 1.8×10^{-2} M in order to examine the influence of [SLS] on the initial rate (V_i). The plot in Fig. 2 demonstrates that the reaction rate increases as the concentration of SLS rises, reaching a maximum at 7.85×10^{-3} M, which is close to the critical micelle concentration of SLS. However, beyond this point, a declining pattern in the initial rate is noticed as the concentration of SLS

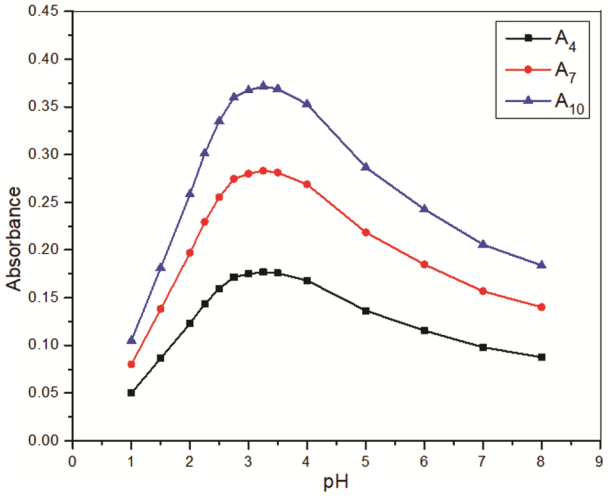

Fig. 1 — The correlation between pH and absorbance at Temperature = 298 ± 0.1 K, [SLS] = 7.85×10^{-3} M, I = 0.05 M ($NaNO_3$), [PHZ] = 5.25×10^{-4} M, $[Pd^{2+}] = 4.5 \times 10^{-5}$ M, and $[Fe(CN)_6^{4-}] = 7.25 \times 10^{-3}$M

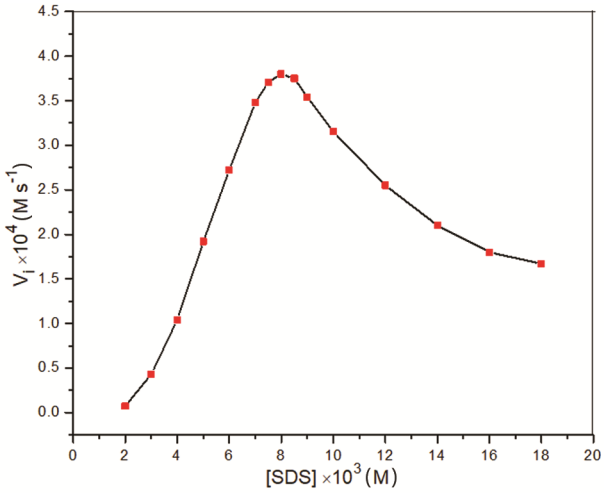

Fig. 2 — The correlation between [SLS] and absorbance at Temperature = 298 ± 0.1 K, [PHZ] = 5.25 × 10^{-4} M, I = 0.05 M ($NaNO_3$), pH = 3.25 ± 0.01, [Pd^{2+}] = 4.5 × 10^{-5} M, and [$Fe(CN)_6^{4-}$] = 7.25 × 10^{-3}M

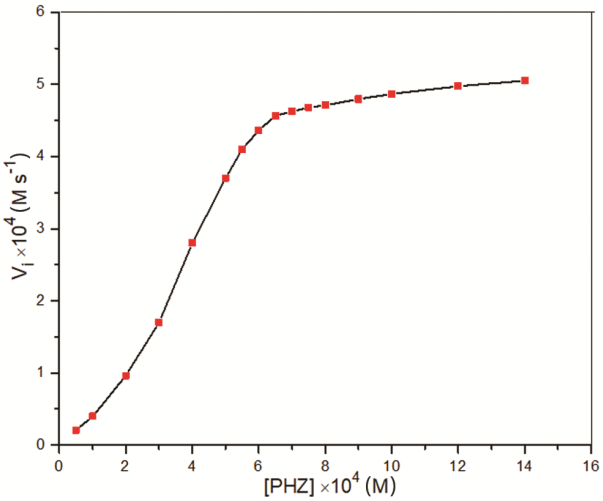

Fig. 3 — The correlation between [PHZ] and initial rate at Temperature = 298 ± 0.1 K, [SLS] = 7.85 × 10^{-3} M, I = 0.05 M ($NaNO_3$), pH = 3.25 ± 0.01, [Pd^{2+}] = 4.5 × 10^{-5} M, and [$Fe(CN)_6^{4-}$] = 7.25 × 10^{-3}M

continues to increase within the range studied. At 7.85 x 10^{-3} M [SLS], which is somewhat less than the stated CMC for aqueous SLS, the highest reaction rate was found. The CMC of SLS in the current reaction conditions can be determined by plotting the initial rate versus the [SLS]. By finding the point where the two straight lines intersect, one with a positive slope and the other with a negative slope, the CMC of SLS is determined to be 7.85 x 10^{-3} M. This value is a bit lower compared to the disclosed CMC of SLS in an aqueous medium[15]. At or near the CMC of SLS, the reaction occurs partially on a micellar interface and partially in the aqueous phase[45].

Understanding the factors that influence reaction rates in a micellar medium involves considering the spatial distribution of reactants in the micellar and aqueous pseudophases. It is important to note that reactants may exhibit distinct response rates in the two aforementioned pseudophases[46]. When the concentration of surfactant is below the critical micelle concentration, the individual surfactant molecules function as catalysts, leading to an increase in the reaction rate with [Surfactant]. Catalytic micelle formation can occur through an association of surfactant monomers with substrate molecules. This aggregation promotes the reaction and enhances the reaction rate. Research in literature demonstrates that the reaction rate in the presence of surfactants is also affected by the premicellar region[47, 48]. The reactivity of the substrates in the micellar aggregate is lower than that of the substrate in premicellar complexes[49]. Once the premicellar complexes disintegrate and micelle formation occurs, the reaction rate ceases after attaining its maximum point at the CMC. An inverse relationship between the reaction rate and the [SLS] was observed after the CMC of the SLS. It is noteworthy to highlight that the aqueous surface exhibits significantly higher polarity than the micellar surface. Hence, the apparent reduction in the reaction rate could be attributed to either the partitioning of the substrate among aqueous and micellar pseudophases or the diminished electrical conductivity of the medium[49]. In addition, the introduction of surfactant beyond the CMC resulted in a decrease in reaction rate due to the potential dilution of the approaching ligand[50].

Influence of varying [PHZ] on the initial rate

The influence of variable [PHZ] on the initial rate was investigated at a temperature of 298 K within the range of 0.5 × 10^{-4} to 14.0 × 10^{-4} M under the optimal pH conditions. The graph depicting the relationship between the initial rate and [PHZ] (Fig. 3) illustrates a sharp rise in the substitution rate up to 6.5 × 10^{-4} M [PHZ]. The reaction rate increase very slowly with additional increase in [PHZ] up to 14.0 × 10^{-4} M. The CN^- concentration in the reacting mixture will exhibit an upward trend as the [PHZ] increases, facilitated by the liberation of CN^- from $[Fe(CN)_6]^{4-}$. The constancy in initial rate observed at higher [PHZ] levels can be ascribed to the lower effective concentration of Pd^{2+} due to the emergence of the complex involving Pd^{2+} and CN^-[29]. The PHZ

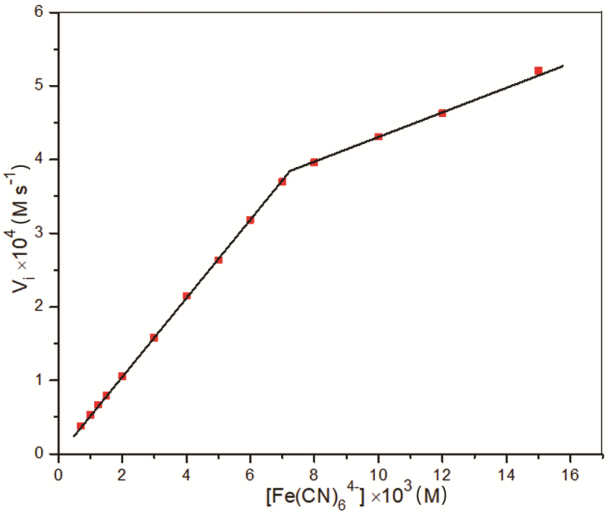

Fig. 4 — The correlation between $[Fe(CN)_6^{4-}]$ and initial rate at Temperature = 298 ± 0.1 K, [SLS] = 7.85 × 10^{-3} M, I = 0.05 M ($NaNO_3$), [PHZ] = 5.25 × 10^{-4} M, pH = 3.25 ± 0.01, and $[Pd^{2+}]$ = 4.5 × 10^{-5} M

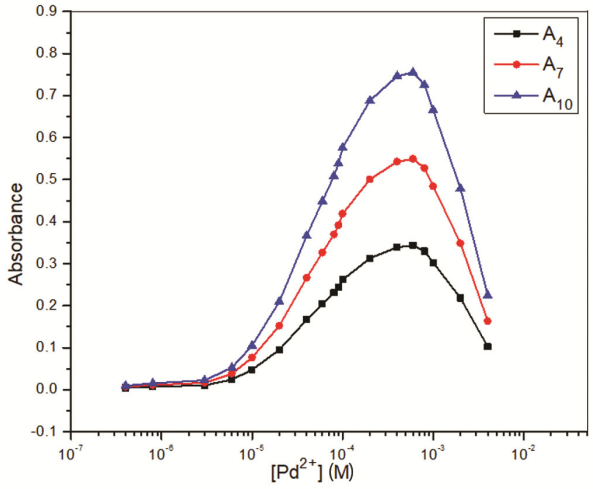

Fig. 5 — The correlation between $[Pd^{2+}]$ and Absorbance at $[Fe(CN)_6^{4-}]$ = 7.25 × 10^{-3}M, Temperature = 298 ± 0.1 K, [SLS] = 7.85 × 10^{-3} M, I = 0.05 M ($NaNO_3$), [PHZ] = 5.25 × 10^{-4} M, pH = 3.25 ± 0.01, and $[Pd^{2+}]$ = 4.5 × 10^{-5} M

makes a complex with Pd^{2+} ions, resulting in a reduction of its actual concentration. The comparative lower reaction rate observed at higher [PHZ] concentrations can also be ascribed to the decreased efficacy of the Pd^{2+} catalyst[42].

Influence of varying $[Fe(CN)_6]^{4-}$ on the initial rate

The initial rate was determined by utilizing the optimal conditions of [PHZ] and pH while holding all other reaction parameters unchanged. The computation of the initial rate was performed with reference to $[Fe(CN)_6^{4-}]$ within the 0.7 × 10^{-3} to 15.0 × 10^{-3} M concentration range. Based on the calculated initial rate (V_i) for each $[Fe(CN)_6^{4-}]$, as shown in Fig. 4, it is apparent that the tested spectrum of $[Fe(CN)_6^{4-}]$ demonstrates a variable order kinetics. At a lower $[Fe(CN)_6]^{4-}$ levels, the indicator reaction implements first-order kinetics. While, when $[Fe(CN)_6^{4-}]$ surpasses 7.0 × 10^{-3} M, the order of the reaction decreases from unity.

Influence of varying $[Pd^{2+}]$ on the initial rate

Considering the potential application of Pd^{2+}-catalyzed substitution reactions for the detection of Pd^{2+} at low concentrations, it is crucial to examine the influence of $[Pd^{2+}]$ on the substitution rate. The study focused on examining the reaction rate within the range of 4.0 × 10^{-7} to 4.0 × 10^{-3} M $[Pd^{2+}]$ under the most favourable reaction conditions. This was achieved by measuring the absorbance at specific time intervals (4, 7, and 10 min after initiation of reaction) as a means to determine the initial rate at varying concentrations of $[Pd^{2+}]$. A direct correlation was observed between the absorbance and $[Pd^{2+}]$ concentration at low levels of Pd^{2+}. In Fig. 5, it can be observed that the absorbance/reaction rate exhibits a nonlinear progression until the concentrations of the catalyst and the iron complex reach a point of comparability. The rapid increase of the reaction rate up to 6.0 × 10^{-4}M $[Pd^{2+}]$ could potentially be attributed to the formation of a binuclear adduct between $[Fe(CN)_6]^{4-}$ and Pd^{2+}[28, 41]. The resulting binuclear adduct undergoes swift isomerization in an aqueous medium, leading to the formation of the catalyst in the form of $PdCN^+$ and a more reactive $[Fe(CN)_5H_2O]^{3-}$. An increase in $[Pd^{2+}]$ leads to enhanced complexation amongst Pd^{2+} and $[Fe(CN)_6]^{4-}$, resulting in a reduction in the catalyst's effective concentration and subsequently causing a significant decline in the substitution rate[27, 28].

Impact of ionic strength and temperature on the initial rate

The influence of ionic strength, I, on the initial rate was also investigated by controlling the reaction media's ionic strength between 0.05-0.40 M with sodium nitrate. Fig. 6 shows a negative salt effect in V_i versus ionic strength (I). Na^+ of $NaNO_3$ electrostatically interacts with CN^- to lower metal center electron density. Decreased electron density makes eliminating water from $[Fe(CN)_5\ H_2O]^{3-}$ challenging, resulting in a reduction in reaction rate with rising ionic strength. Subsequently, an ionic strength of 0.05 M was chosen for subsequent investigation due to its ability to induce a significant alteration in the absorbance value.

Temperature effects on sensitivity were investigated within a 20-40°C range. Researchers also looked at the reaction at higher temperatures and discovered that the complex, $[Fe(CN)_5\ PHZ]^{3-}$, degrades when exposed to elevated temperatures. As anticipated, the reaction adhered to the Arrhenius equation, indicating that the reaction rate escalates as the temperature increases. At a temperature of 25°C, the reaction exhibits a fair rate of progression. Thus, it is suggested that a temperature of 298K would be the optimal choice for conducting further research on the indicator reaction system.

Procedure for the assay of pure Biotin

The calibration graphs for the analytical quantification of BTN was established by varying its concentration within the range of 0.010-1.954 µg mL^{-1} while maintaining optimal reaction conditions: Temperature = 298 ± 0.1 K, [SLS] = 7.85 × 10^{-3} M, I = 0.05 M ($NaNO_3$), [PHZ] = 5.25× 10^{-4} M, pH = 3.25 ± 0.01, $[Pd^{2+}]$ = 4.5 × 10^{-5} M, and $[Fe(CN)_6^{4-}]$ = 7.25 × 10^{-3} M. The relationship between the [BTN] and absorbance at fixed time (4, 7, and 10 min), using the linear least-squares treatment was observed to be linear within the band of concentrations under investigation (Fig. 7). Based on the experimental findings, the optimal time intervals of 4, 7, and 10 min were selected due to their superior sensitivity and correlation coefficient, as indicated in Table 2. The figures of merit i.e. the values of slope (b), intercept (a), correlation coefficient (r), and sensitivity are given in Table 2. Hence, the concentration of BTN can be determined by employing the calibration/regression equation A_t = b [BTN] + a, where a and b represent the intercept and slope, respectively, and A_t denotes the absorbance measured at specific time intervals (t = 4, 7, and 10 min).

The accuracy of the approach suggested was validated through multiple individual measurements for the retrieval of BTN from solutions with different concentrations, employing the A_4 calibration curve under optimal conditions. The findings are presented in Table 3. The experimental recoveries, when comparing the detected concentrations to the injected concentrations within the calibrated range, varied between 98% and 101%. The threshold for detection of BTN was established as 0.117 µg mL^{-1}.

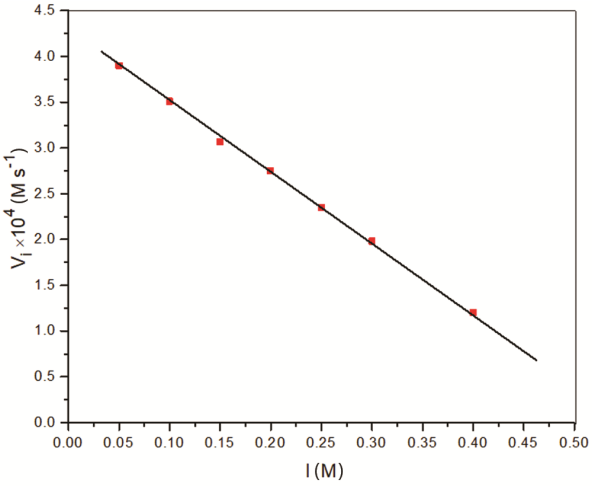

Fig. 6 — The correlation between Ionic strength and initial rate at $[Fe(CN)_6^{4-}]$ = 7.25 × 10^{-3}M, Temperature = 298 ± 0.1 K, [SLS] = 7.85 × 10^{-3} M, I = 0.05 M ($NaNO_3$), [PHZ] = 5.25 × 10^{-4} M, pH = 3.25 ± 0.01, and $[Pd^{2+}]$ = 4.5 × 10^{-5} M

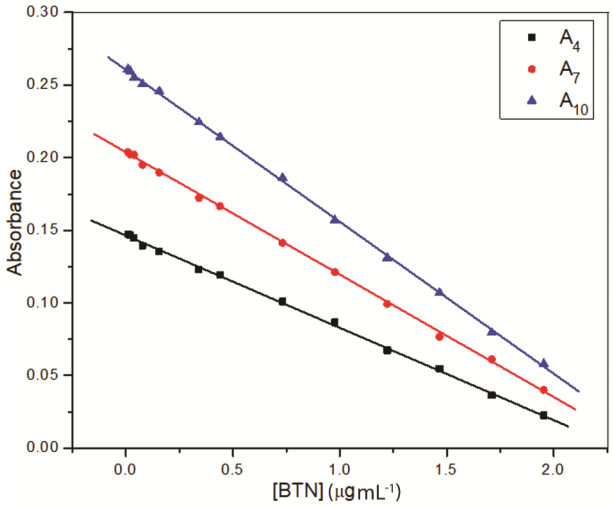

Fig. 7 — Linear regression calibration plots at fixed times, t = 3, 5 and 8 minutes under the condition: $[Fe(CN)_6^{4-}]$ = 7.25 × 10^{-3}M, Temperature = 298 ± 0.1 K, [SLS] = 7.85 × 10^{-3} M, I = 0.05 M ($NaNO_3$), [PHZ] = 5.25 × 10^{-4} M, pH = 3.25 ± 0.01, and $[Pd^{2+}]$ = 4.5 × 10^{-5} M

Table 2 — Regression equations, sensitivity, and correlation coefficient of calibration graphs at fixed times under optimized conditions: $[Fe(CN)_6^{4-}]$ = 7.25 × 10^{-3}M, Temperature = 298 ± 0.1 K, [SLS] = 7.85 × 10^{-3} M, I = 0.05 M ($NaNO_3$), [PHZ] = 5.25 × 10^{-4} M, pH = 3.25 ± 0.01, and $[Pd^{2+}]$ = 4.5 × 10^{-5} M

Time (min)	[BTH] (µg mL^{-1})	Regression/Calibration equation	Correlation coefficient	Sensitivity
4	0.010-1.954	0.630 × 10^5 [BTH] + 0.1464	0.9979	0.630 × 10^5
7	0.010-1.954	0.859 × 10^5 [BTH] + 0.2037	0.9992	0.859 × 10^5
10	0.010-1.954	1.053 × 10^5 [BTH] + 0.2608	0.9984	1.053 × 10^5

The study utilized a redesigned mechanistic approach as shown in Scheme 1 to demonstrate the inhibitory effect of BTN on the Pd^{2+} catalyzed cyanide exchange from $[Fe(CN)_6]^{4-}$ by PHZ. The speculated mechanism bears resemblance to the process catalyzed by an enzyme in the presence of an inhibitor.

Interferences study

Excipients are non-reactive substances employed in pharmaceutical products to serve as preservatives, colouring agents, and fillers alongside their primary medicinal constituents. The proposed approach was evaluated for its potential analytical applications through recovery trials conducted under optimal

Table 3 — Accuracy and precision of the recommended methodology for the determination of BTN at, $[Fe(CN)_6^{4-}] = 7.25 \times 10^{-3}$M, Temperature = 298 ± 0.1 K, [SLS] = 7.85×10^{-3} M, I = 0.05 M ($NaNO_3$), [PHZ] = 5.25×10^{-4} M, pH = 3.25 ± 0.01, and $[Pd^{2+}] = 4.5 \times 10^{-5}$ M

BTH added (μg mL^{-1})	BTH found[a] (μg mL^{-1})	Recovery (%)	Error (%)
0.019	0.0193 ± 0.03	101.6	+ 1.57
0.039	0.0395 ± 0.04	101.3	+ 1.28
0.078	0.077 ± 0.02	98.7	- 1.28
0.156	0.155 ± 0.06	99.4	- 0.64
0.342	0.344 ± 0.04	100.6	+ 0.58
0.440	0.448 ± 0.04	101.8	+ 1.81
0.733	0.741 ± 0.02	101.1	+ 1.09
0.977	0.969 ± 0.06	99.2	- 1.22
1.222	1.216 ± 0.12	99.5	- 0.49
1.466	1.473 ± 0.03	100.5	+ 0.48
1.710	1.722 ± 0.08	100.7	+ 0.70
1.954	1.941 ± 0.04	99.3	- 0.67

[a]Average of three determinations

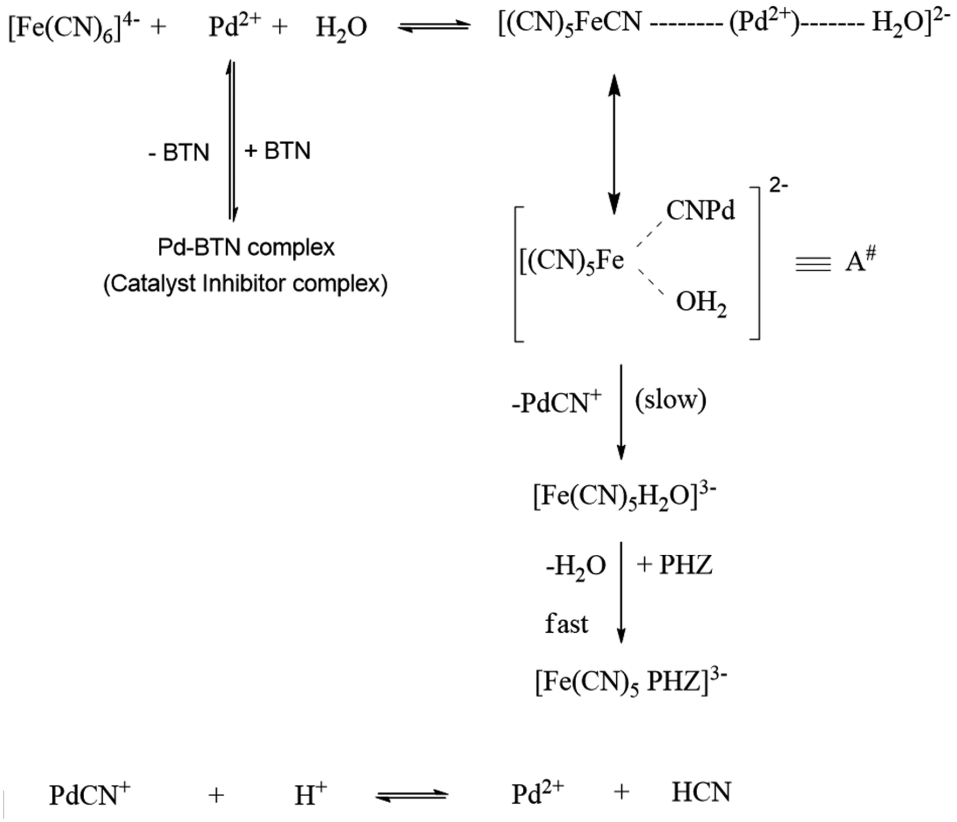

Scheme 1 — Mechanism for Pd^{2+} catalyzed cyanide exchange from $[Fe(CN)_6]^{4-}$ by PHZ

Table 4 — Findings from BTN recovery experiments conducted with common excipients at: $[Fe(CN)_6^{4-}] = 7.25 \times 10^{-3}$ M, Temperature = 298 ± 0.1 K, [SLS] = 7.85×10^{-3} M, I = 0.05 M ($NaNO_3$), [PHZ] = 5.25×10^{-4} M, pH = 3.25 ± 0.01, and $[Pd^{2+}] = 4.5 \times 10^{-5}$ M

Excipients	Amount taken (µg)	INH found[a] (µg)	Recovery (%)
Oxalate	45	0.446	99.1 ± 0.9
Stearate	45	0.444	98.6 ± 0.5
Gelatin	45	0.447	99.3 ± 0.3
Dextrose	45	0.453	100.7 ± 0.5
Citrate	45	0.455	101.1 ± 0.8
Glucose	45	0.448	99.6 ± 0.6
Nicotinamide	45	0.457	101.6 ± 0.4
Starch	45	0.460	102.2 ± 0.6
Lactose	45	0.444	98.7 ± 0.6

[a]Average of three determinations

Table 5 — Comparative analysis of BTN quantification in pharmaceutical samples with official method at: $[Fe(CN)_6^{4-}] = 7.25 \times 10^{-3}$M, Temperature = 298 ± 0.1 K, [SLS] = 7.85×10^{-3} M, I = 0.05 M ($NaNO_3$), [PHZ] = 5.25×10^{-4} M, pH = 3.25 ± 0.01, and $[Pd^{2+}] = 4.5 \times 10^{-5}$ M

Drug (Tablets)	Proposed Approach [Recovery ± SD (%)]	Standard Approach [Recovery ± SD (%)]
Biosort-5, 5 mg Tablet (Consern Pharma Ltd, Punjab, India)	99.83 ± 0.53	100.81 ± 0.78
VB-7 5 mg Tablet (Intas Pharmaceutical Ltd. Sikkim, India)	100.56 ± 0.68	101.13 ± 0.61
Boit-5, 5 mg Tablet (Premier Medical Agency, Maharashtra, India)	99.79 ± 0.77	99.91 ± 0.56
Essvit, 5 mg Tablet (Sun Pharmaceuticals Ind. Ltd. Mumbai, India)	99.39 ± 0.68	100.42 ± 0.82
Biotal-10, 10 mg Tablet (Cosmederma, Haryana, India)	98.83 ± 0.92	99.64 ± 0.66
H-Vit, 5 mg Tablet (Systopic Laboratories Pvt. Ltd., New Delhi, India)	101.13 ± 0.34	99.68 ± 0.39
Treslong-5, 5 mg Tablet (Allwell Healthcare Solutions, Amravati, India)	102.27 ± 0.57	100.93 ± 0.73

[a]Average of three determinations

reaction settings, which involved the use of 0.45 µg of BTN and a 100-fold concentration of common excipients. The A_4 calibration model was employed for this evaluation. The obtained findings indicate that the incorporation of commonly used additives in pharmaceutical products does not exert a substantial influence on the quantification of BTN using the suggested methodology, despite their presence being 100 times greater than that of BTN (Table 4).

Quantification of BTN in medicinal formulations

Weighing the biotin tablets allowed us to calculate their average mass per tablet. After being precisely weighed, a fraction of the final product corresponding to 100 mg of BTN was added to a 100 mL standardized flask that held 70 mL of doubled distilled water. The flask's contents were subjected to sonication for approximately 15 min, followed by the addition of de-ionized water to reach a final volume of 100 mL. Finally, the solution underwent filtration using a Whatmann filter paper (0.45 µm Milli-pore). The drug's intended concentrations were achieved through precise dilutions using double distilled water. The analysis of the solution was conducted directly, utilizing the calibration model developed in accordance with the aforementioned procedure for the quantification of pure BTN, without requiring any extraction or pretreatment procedures.

The analysis of BTN content was performed on seven distinct pharmaceutical samples, and the findings are displayed in Table 5. A statistical comparison was made between the results and the standard approach in terms of accuracy and precision. The outcomes of the developed method for determining BTN were found to be highly congruent with those of the standard approach[51]. The average recoveries ranged from 98% to 102%, indicating that the developed approach is likely suitable for rapidly determining BTN in pharmaceutical products.

Conclusion

The authors have successfully developed a ligand-substitution-kinetic spectrophotometric method that is precise, sensitive, swift, cost-efficient, and practical for quantifying BTN. This approach utilizes the inhibitory effect of BTN on the Pd^{2+} catalyzed ligand exchange reaction involving PHZ and $[Fe(CN)_6]^{4-}$. The technique was utilized to quantify BTN in drug samples, and the outcomes exhibited a strong correlation with those derived from the standard approach. The proposed methodology offers several

advantages compared to various spectrophotometric techniques. It eliminates the need for extraction, heating, and the use of oxidants, organic dyes, or catalysts, thereby reducing potential sources of inaccuracy in the measurement of BTN. The data from the restoration study has unambiguously confirmed the method's accuracy and repeatability. The proposed LS-kinetic assay is highly suitable for the quantification of BTN in pharmaceutical formulations and has the potential to decrease the time required for analysis. Hence, the suggested approach can be effectively utilized for regular auditing of the biotin and other medications. This approach is extremely efficient for precisely determining trace levels of a variety of drugs and biological molecules that have the potential to significantly hinder the catalytic activity of Pd(II).

References

1 B S & Strand T A, Biotin: A scoping review for nordic nutrition recommendations, *Food Nutr Res*, 68 (2024) 10256.

2 Almohanna H M, Ahmed A A & Tsatalis J P, The role of vitamins and minerals in hair loss: A review, *Dermatol Ther*, 9 (2019) 51.

3 Satiaputra J, Shearwin K E, Booker G W & Polyak S W, Mechanisms of biotin-regulated gene expression in microbes, *Synth Syst Biotechnol*, 1 (2016) 17.

4 Wal A, Sasmal A, Singh R, Yadav P, Singh Y, Garg V & Wal P, Regulatory role, mechanism, and metabolic profile of Biotin in gene expression, *Curr Pharmacogenomics Per Med*, 20 (2023) 73.

5 Ofoedu C E, Iwouno J O, Ofoedu E O, Ogueke C C, Igwe V S, Agunwah I M, Ofoedum A F, Chacha J S, Muobike O P, Agunbiade A O, Njoku N E, Nwakaudu A A, Odimegwu N E, Ndukauba O E, Ogbonna C U, Naibaho J, Korus M & Okpala C O R, Revisiting food-sourced vitamins for consumer diet and health needs: A perspective review, from vitamin classification, metabolic functions, absorption, utilization, to balancing nutritional requirements, *Peer J*, 9 (2021) e11940.

6 Patel D P, Swink S M & Castelo-Soccio L, A Review of the use of biotin for hair loss, *Skin Appendage Disord*, 3 (2017) 166.

7 Oca M, Gutiérrez-Ospina G, Salcedo P, Fuentes-Farías A, Meléndez-Herrera E, Gómez-Chavarín M & Báez-Saldaña A, Differential effect of biotin on carboxylase activity and mice skeletal muscle metabolism, *Adv Biosci Biotechnol*, 4 (2013) 43.

8 Dakshinamurti K, Dakshinamurti S & Czubryt M P, Effects of biotin deprivation and biotin supplementation In: Preedy V & Patel V, (Eds) *Handbook of Famine, Starvation, and Nutrient Deprivation* (Springer, Cham) 2017.

9 Watkins B A, Influences of biotin deficiency and dietary trans-fatty acids on tissue lipids in chickens, *Br J Nutr*, 61 (1989) 99.

10 Mukhopadhyay D, Das M K, Dhar S & Mukhopadhyay M, Multiple carboxylase deficiency (late onset) due to deficiency of biotinidase, *Indian J Dermatol*, 59 (2014) 502.

11 Zempleni J, Hassan Y I & Wijeratne S S, Biotin and biotinidase deficiency, *Expert Rev Endocrinol Metab*, 3 (2008) 715.

12 Sekhon B S, Surfactants: Pharmaceutical and medicinal aspects, *J Pharm Technol Res Manag*, 1 (2013) 43.

13 Das B, Kumar B, Begum W, Bhattarai A, Mondal M H & Saha B, Comprehensive review on applications of surfactants in vaccine formulation, therapeutic and cosmetic pharmacy and prevention of pulmonary failure due to COVID-19, *Chem Afr*, 5 (2022) 459.

14 Shah S, Chatterjee S K & Bhattarai A, The effect of methanol on the micellar properties of dodecyltrimethylammonium bromide (DTAB) in aqueous medium at different temperatures, *J Surfactants Deterg,* 19 (2016) 201.

15 Motin A, Hafiz-Mia M A & Nasimul-Islam A K M, Thermodynamic properties of sodium dodecyl sulfate aqueous solutions with methanol, ethanol, n-Propanol and iso-Propanol at different temperatures, *J Saudi Chem Soc*, 19 (2015) 172.

16 Mukerjee P, Size distribution of small and large micelles: Multiple equilibrium analysis, *J Phys Chem*, 76 (1972) 565.

17 Rauf A, Baloch M K, Khan A, Khan Z & Rauf S, Effect of concentration and molecular mass of peo on the micellization and thermodynamic behaviour of cetyltrimethylammonium bromide (CTAB) in aqueous peo-ctab mixed system, *J Chil Chem Soc*, 61 (2016) 3013.

18 Tang K, Chemical diversity and biochemical transformation of biogenic organic sulfur in the ocean, *Front Mar Sci*, 7 (2020) 68.

19 Abadie C & Tcherkez G, Plant sulphur metabolism is stimulated by photorespiration, *Commun Biol*, 2 (2019) 379.

20 Kolluru G K, Shen X & Kevil C G, Reactive sulfur species, a new redox player in cardiovascular pathophysiology, *Arterioscler Thromb Vasc Biol*, 40 (2020) 874.

21 Srivastava A, Manjusha, Srivastava N & Naik R M, Kinetic study of Ru(III) promoted oxidation of L-tryptophan in an anionic surfactant medium by hexacyanoferrate(III), *J Mex Chem Soc,* 67 (2023) 46.

22 Iioka T, Takahashi S, Yoshida Y, Matsumura Y, Hiraoka S & Sato H, A kinetics study of ligand substitution reaction on dinuclear platinum complexes, stochastic versus deterministic approach, *J Comput Chem*, 40 (2019) 279.

23 Srivastava A, Singh R, Srivastava N & Naik R M, Kinetic study of Ru(III)-catalyzed oxidation of L-phenylalanine by hexacyanoferrate(III) in an anionic surfactant medium, *Tenside Surfactants Deterg*, 60 (2023) 376.

24 Srivastava A, Sharma V, Prajapati A, Srivastava N & Naik R M, Spectrophotometric determination of ruthenium utilizing its catalytic activity on oxidation of hexacyano ferrate(II) by periodate ion in water samples, *Chem Chem Technol*, 13 (2019) 275.

25 Srivastava A, Srivastava N & Srivastava K, Cu(II) catalyzed oxidation of L-phenylalanine in cationic micellar medium, *S Afr J Chem*, 77 (2023) 143.

26 Srivastava A, Srivastava N & Singh R, Determination of alpha-lipoic acid in pharmaceutical samples using inhibitory kinetic approach in SLS micellar medium, *Indian J Chem*, 62 (2023) 931.

27 Srivastava A, Quantitative estimation of D-penicillamine in pure and pharmaceutical samples using inhibitory kinetic spectrophotometric method, *Biointerface Res App Chem*, 11 (2021) 16654.

28 Srivastava A, Srivastava N, Srivastava K, Naik R M & Srivastava A, Inhibitory kinetic approach for the rapid micro-level quantification of N-acetylcysteine, *Russ J Phys Chem*, 96 (2022) 3082.

29 Srivastava A, Sharma V, Singh V K & Srivastava K, A simple and sensitive inhibitory kinetic method for the carbocisteine determination, *J Mex Chem Soc*, 66 (2022) 57.

30 Srivastava A & Srivastava K, A simple and sensitive inhibitory kinetic method for the methionine determination, *Phys Chem Res*, 10 (2022) 283.

31 Pérez-Ruiz T, Martínez-Lozano C & Sanz A, Electrophoretic behaviour of biotin and biocytin in capillary electrophoresis determination of biotin in pharmaceutical formulations, *Chromatographia*, 58 (2003) 757.

32 Livaniou E, Costopoulou D, Vassiliadou I, Leondiadis L, Nyalala J O, Ithakissios D S & Evangelatos G P, Analytical techniques for determining biotin, *J Chromatogr*, 881 (2000) 331.

33 Chastain J L, Bowers-Komro D M & McCormick D B, High-performance liquid chromatography of biotin and analogues, *J Chromatogr*, 330 (1985) 153.

34 Crivelli S L, Quirk P F & Steible D J, A reversed-phase high-performance liquid chromatographic (HPLC) assay for the determination of biotin in multivitamin-multimineral preparations, *Pharm Res*, 4 (1987) 261.

35 Yokoyama T & Kinoshita T, High-performance liquid chromatographic determination of biotin in pharmaceutical preparations by post-column fluorescence reaction with thiamine reagent, *J Chromatogr*, 542 (1991) 365.

36 Gadzala-Kopciuch R, Szumski M & Buszeski B, Determination of biotin in pharmaceutical preparations by means of HPLC and/or MECK, *J Liq Chromatogr Rel Technol*, 26 (2023) 195.

37 Walash M I, Rizk M, Sheribah Z A & Salim M M, Kinetic spectrophotometric determination of biotin in pharmaceutical preparations, *Int J Biomed Sci*, 4 (2008) 238.

38 Sevgi T U, Spectrofluorimetric determination and validation of biotin in pure and dosage form via derivatization with 4-fluoro-7-nitrobenzofurazan, *Chin J Chem*, 28 (2010) 2209.

39 Ekpe A E & Hazen C, Liquid chromatographic determination of biotin in multivitamin-multimineral tablets, *J Pharm Biomed Anal*, 16 (1998) 1311.

40 Gröningsson K & Jansson L, TLC determination of biotin in a lyophilized multivitamin preparation, *J Pharm Sci*, 68 (1979) 364.

41 Srivastava A, Singh V K & Srivastava N, Kinetic study of Hg(II)-promoted cyanide substitution from hexacyanoferrate(II) in an anionic surfactant medium by N-R-Salt, *Russ J Phys Chem*, 97 (2023) 587.

42 Naik R M, Tiwari P K, Singh P K & Yadav S B S, The silver(I)-catalyzed exchange of coordinated cyanide in hexacyanoferrate(II) by phenylhydrazine in aqueous medium, *Int J Chem Kinet*, 39 (2007) 447.

43 Perrin D D & Sayce I G, Computer calculation of equilibrium concentrations in mixtures of metal ions and complexing species, *Talanta*, 14 (1967) 833.

44 Ivanov V M, Mamedova A M & Figurovskaya V N, Photometric, colorimetric, and acid-base characteristics of nitroso-R-salt, *J Anal Chem*, 61 (2006) 571.

45 Naik R M & Kumar B, Kinetics and mechanism of formation of [Fe (CN) 5D-PA] 3-by ligand substitution reaction in the presence of surfactant micelle in acidic media, *J Disper Sci Technol*, 33 (2012) 647.

46 Brinchi L, Di-Profio P, Germani R, Savelli G, Tugliani M & Bunton C A, Hydrolyses of dinitroalkoxyphenyl phosphates in aqueous cationic micelles acceleration by premicelles, *Langmuir*, 16 (2000) 10101.

47 Lopez-Cornejo P, Mozo J D, Roldán E, Domınguez M & Sanchez F, Kinetic study of the reaction*$[Ru(bpy)_3]^{2++}$ $S_2O_8^{2-}$ in solutions of Brij-35 at premicellar and micellar concentrations, *Chem Phys Lett*, 352 (2002) 33.

48 Piszkiewicz D, Cooperativity in bimolecular micelle-catalyzed reactions inhibition of catalysis by high concentrations of detergent, *J Am Chem Soc*, 99 (1977) 7695.

49 Sen P K, Gani N & Pal B, Effects of microheterogeneous environments of SDS, TX-100, and tween 20 on the electron transfer reaction between l-Leucine and $AuCl_4^-/AuCl_3(OH)^-$, *Ind Eng Chem Res*, 52 (2013) 2803.

50 Bunton C A, Nome F, Quina F H & Romsted L S, Ion binding and reactivity at charged aqueous interfaces, *ACC Chem Res*, 24 (1991) 357.

51 The National Formulary 25. Rockville, M D: US Pharmacopeial Convention; The United States Pharmacopoeia 30, Online (2007).